*J. Phys. Chem. B* **2004,** *108,* 5217−5220

# Chemical Bonding in Polyethylene−Nanotube Composites: A Quantum Mechanics Prediction

**K. Mylvaganam and L. C. Zhang***

*School of Aerospace, Mechanical & Mechatronic Engineering, The University of Sydney, NSW 2006, Australia*

*Received: November 26, 2003; In Final Form: February 24, 2004*

To make full use of the strength of carbon nanotubes in a composite, it is important to have a high-stress transfer at the matrix−nanotube interface via strong chemical bonding. This paper investigates the possible polyethylene−nanotube bonding with the aid of a quantum mechanics analysis. The polyethylene chains were represented by alkyl segments, and the nanotubes were modeled by nanotube segments with H atoms added to the dangling bonds of the perimeter carbons. The study predicts that covalent bonding between an alkyl radical and a nanotube is energetically favorable, and that the tubes of smaller diameters have higher binding energies. Hence, a high-stress transfer can be realized in polyethylene-based carbon nanotube composites in the presence of free-radical generators.

## 1. Introduction

Polymer-based composites reinforced by carbon fibers have been widely used in advanced structures. Compared to the fibers, carbon nanoubes have many superior mechanical properties such as elastic moduli of 1−5 TPa and fracture strain of 10−100 times better. In addition, their aspect ratio is much greater, which is preferable in making a stronger composite. As such, carbon nanotubes are being considered in place of fibers for reinforcing polymers. Some experimental works have been reported on various polymer−nanotube composites.[1−11] However, the reports on the relevant properties of the composites have been confusing and very often conflicting. For example, Ren et al.[5] studied the tension−tension fatigue behavior of unidirectionally aligned single-wall nanotube (SWNT) reinforced epoxy composite and found that SWNT ropes have good potential as reinforcement in fatigue-resistant, high-fracture toughness polymer composites. Bower et al.[6] investigated the composite of uniaxially oriented multiwall nanotube (MWNT) embedded in a thermoplastic polymer, poly hydroxy amino ether. They stretched the composite until fracture and observed a high density of protruding nanotubes having ball-like masses of polymer near the tip of the tube showing the adherence of polymer to the nanotubes. On the other hand, Lau and Hui[10] found that the use of MWNT for advanced composite structures may not improve the mechanical strength of the structures. Lau and Shi[11] found that the bending stiffness of the nanotube composite beam is grater than that of pure epoxy while the maximum flexural strengths are lower.

Polyethylene is one of the simplest among the well-studied polymers with a known crystal structure and has a wide range of applications. Early experimental work[2] on polyethylene−nanotube composites showed that an increase in the aspect ratio of the naotubes would bring about an enhanced strength and stiffness of the composite. Recently, Ruan et al.[3] reported that the presence of MWNT in polyethylene led to an increase in strain energy density, ductility, and tensile strength and attributed these to the chain mobility enhancement in ultrahigh molecular weight polyethylene (UHMWPE) induced by the MWNTs. Tang et al.[4] found an increase in the stiffness, the yield strength, and the fracture toughness of high-density polyethylene (HDPE) composite films with increasing MWNT content. Owing to its simplicity, polyethylene−nanotube composites have also been studied theoretically to a certain extent using the molecular dynamics simulation.[12−15] These studies discussed the effect of chemical bonds and nonbonded interactions, between the polymer chains and nanotubes, on short and long SWNT's. On the effect of chemical bonds, they artificially created bonds between nanotube and polymer chains by introducing two methylene cross-linked units. Nevertheless, the theoretical rationale for the chemical bonding was not verified. The best experimental evidence for chemical modification of carbon nanotube sidewalls is the reaction with fluorine to form stable fluorinated products.[16,17] Bauschlicher[18,19] and Jaffe[20] have independently studied the addition of H atoms and F atoms to the nanotube sidewall by the ab initio computational chemistry approach, and they obtained results that are in agreement with experimental data.

The work of Patil and Brois[21] on fullerene-grafted hydrocarbon polymers is of interest. In this work, they first heated a mixture of fullerene and ethylene butylene copolymer to 150 °C and then added *tert*-butyl peroxide. From the infrared spectroscopy and gel permeation chromatography results, they speculated the existence of an average of six polymer chains free radically grafted on to fullerene.

Since carbon nanotubes are fullerene-related structures, it may be possible to form chemical bonds between nanotube and polyethylene chains using free-radical generators such as peroxide. In principle, radicals can be generated on polyethylene chains either by the abstraction of a hydrogen atom attached to the polymer backbone or by the cleavage of the backbone to yield terminal radicals. The former is frequently encountered as a result of chemical or radiation attack. For example, an oxy radical generated by homolysis of peroxide is capable of abstracting a hydrogen atom from a polyethylene chain and thereby generating a radical. Depending on the hydrogen that is removed, the radical site could be anywhere on the polymer chain. The backbone cleavage is generally caused by severe

---

* To whom correspondence may be addressed. E-mail: zhang@aeromech.usyd.edu.au.

10.1021/jp037619i CCC: $27.50

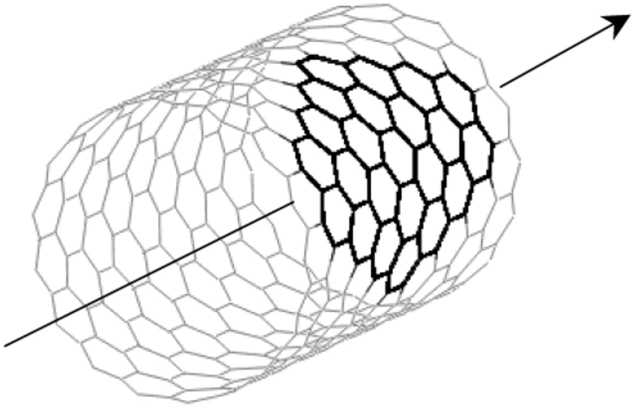

**Figure 1.** A segment of the (17,0) carbon nanotube showing the polycyclic rings of $C_{64}H_{20}$ used in model IV.

physical deformation in the molten state under conditions of extreme shear. For example, in the reported experimental works, the nanotube−polymer mixture is first stretched at or above the melting temperature of the polymer in order to have a uniform dispersion of the nanotubes. During this process, radicals can be generated by carbon−carbon bond cleavage.

In this work, we will use density functional theory (DFT) to study the possible chemical bond formation between a model polyethylene chain radical and a model nanotube. As these calculations are computationally infeasible on large segments, we will use alkyl radicals to represent the polyethylene chain radical and a segment of a nanotube or model polycyclic aromatic systems that are constrained to have nonplanar geometries with curvatures of interest to represent the nanotubes. In our calculations, we will use a pentyl radical to represent a chain with a single radical site and a heptyl biradical to represent a chain with multiple radical sites.

## 2. Methodology

Four model structures were generated and investigated. The first model (model I, $C_{60}-C_5H_{11}^{\bullet}$) was a fullerene having 60 carbon atoms and a pentyl radical with an unpaired electron on the third carbon atom. This was selected because it was experimentally known that $C_{60}$ is capable of reacting with alkyl radicals. The second model (model II, $C_{60}H_{10}-C_5H_{11}^{\bullet}$) was a (5,0) nanotube segment having 60 C atoms with hydrogen atoms added to the dangling bonds of the perimeter carbons and a pentyl radical as in model I. The third model (model III, $C_{64}H_{20}-C_5H_{11}^{\bullet}$) was a section of a (17,0) nanotube sidewall consisting of 23 hexagons (as shown in Figure 1) with 20 hydrogen atoms added to the dangling bonds of the perimeter carbons (i.e., $C_{64}H_{20}$) and a pentyl radical as in model I. This nanotube model system is similar to Jaffe's model. The fourth model (model IV, $C_{60}H_{10}-C_7H_{14}^{\bullet\bullet}$) was a (5,0) nanotube segment used in model II and a $C_7H_{14}$ biradical with unpaired electrons on the 2nd and 6th carbon atoms. Geometries of all models were fully optimized using DFT with hybrid functional B3LYP[22−25] and a 3-21G basis set,[26] and the atomic spin densities were analyzed by the Mulliken method.[27] The largest model studied, model III, uses 683 basis functions for the 3-21G geometry optimization. Further reactions of the model IV complex radical with a saturated chain $C_5H_{12}$ or with another alkyl radical ($CH_3^{\bullet}$) were also investigated by optimizing the appropriate reactants and products at the same level.

As the systems considered here are open-shell molecular radicals, the unrestricted formalism was used. The present level of calculation, DFT(UB3LYP)/3-21G, is known to produce reasonable results[28] for bond lengths, bond angles, and bond energies for a wide range of molecules. The computations were carried out on a super computer using the ab initio quantum chemistry package Gaussian03.[29]

**TABLE 1: Alkyl Adduct Binding Energies and the New C−C Bond Lengths with Model Nanotubes**

| fullerene/ nanotube model | alkyl radical | binding energy (kJ/mol) | new C−C/C−H bond length (Å) |
|---|---|---|---|
| $C_{60}$ | $C_2H_5-CH^{\bullet}-C_2H_5$ | 131.2 | 1.593 |
| $C_{60}H_{10}$ | $C_2H_5-CH^{\bullet}-C_2H_5$ | 142.0 | 1.606 |
| $C_{64}H_{20}$ | $C_2H_5-CH^{\bullet}-C_2H_5$ | 30.5 | 1.629 |
| $C_{60}H_{10}$ | $CH_3-CH^{\bullet}-(CH_2)_3-CH^{\bullet}-CH_3$ | 225.5 | 1.629, 1.628 |
| $C_{60}H_{10}-C_7H_{14}^{\bullet\bullet}$ | $CH_3^{\bullet}$ | 232.7 | 1.557 |
| $C_{60}H_{10}-C_7H_{14}^{\bullet\bullet}$ | $H^{\bullet}$ | 288.6 | 1.099 |

## 3. Results and Discussion

The results of the calculations of adduct binding energies and the newly formed C−C bond length for $C_{60}$ and various nanotube models are given in Table 1. The optimized geometry of the $C_{60}-C_5H_{11}$ radical (model I) is presented in Figure 2, showing the newly formed covalent bond having a bond length of 1.593 Å. The three C−C bonds radiating from the substituted $sp^3$ carbon lengthened to 1.55 Å. The binding energy of the complex is found to be 131.2 kJ/mol. It is to be noted that in his work on fluorination of $C_{60}$ and nanotubes, Jaffe[20] found that including polarization functions to the C atom (i.e., using a 6-31G(d) basis set) increases the binding energy of fluorine by ∼38 kJ/mol (9 kcal/mol). In fullerene, the localized nature of the $\pi$ electrons facilitates the reaction.

The optimized geometry of the $C_{60}H_{10}-C_5H_{11}$ radical (model II) is presented in Figure 3. This has a binding energy of 142.0 kJ/mol. Though carbon nanotubes are expected to be less reactive than fullerene molecules, the nanotube segment considered here is of diameter 3.92 Å, and as such, it has a high curvature. This means the trigonal carbon atoms of the nanotube segment are more distorted, and the deformation energy required to change the hybridization of the nanotube C atom from $sp^2$ to $sp^3$ would be low. As a result, the binding energy is comparable to that of the fullerene complex. The optimized geometry of the $C_{64}H_{20}-C_5H_{11}$ radical (model III) is shown in Figure 4. Here the polycyclic hydrocarbon $C_{64}H_{10}$ represents a zigzag (17,0) nanotube with a diameter of 13.2 Å. The curvature of this system is fixed by fixing the peripheral C atoms during the optimization procedure. The newly formed C−C bond length (1.629 Å) is a little longer in comparison to the other models studied here, and the calculated binding energy is only 30.5 kJ/mol. This could be due to the low curvature of the (17,0) tube compared to the (5,0) tube. This shows that the strength of the covalent bond will decrease with the nanotube radii.

The optimized geometry of the triplet $C_{60}H_{10} - C_7H_{14}$ biradical (model IV) is presented in Figure 5, which shows two newly formed covalent bonds with bond lengths of 1.629 and 1.628 Å. This leaves two unpaired electrons on the nanotube, which in principle may pair up or combine with two other polymer chains. We find that the corresponding singlet state had ∼14 kJ/mol higher in energy than the triplet state. In the triplet calculation, the Mulliken spin density analysis showed that the two unpaired electrons are localized at two different C atoms as shown in Figure 5. Although they are separated as much as possible, because of the small system, there would still be some repulsion between these electrons. Our calculated total binding energy is 225.5 kJ/mol. As two new bonds are formed,

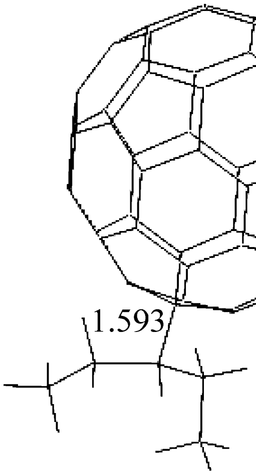

**Figure 2.** DFT(B3LYP)/3-21G-optimized geometry of the $C_{60}-C_5H_{11}$ radical.

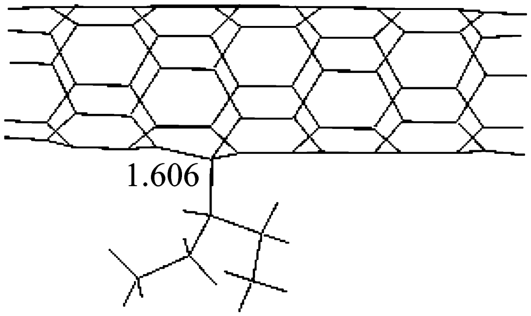

**Figure 3.** DFT(B3LYP)/3-21G-optimized geometry of the $C_{60}H_{10}-C_5H_{11}$ radical.

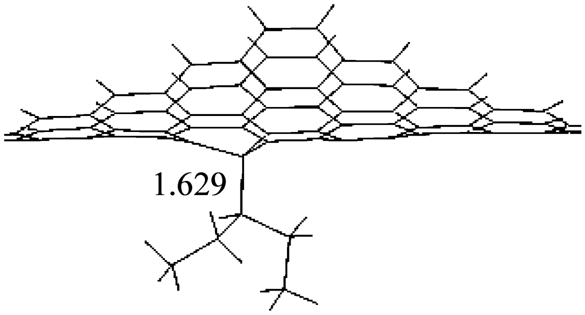

**Figure 4.** DFT(B3LYP)/3-21G-optimized geometry of the $C_{64}H_{20}-C_5H_{11}$ radical.

the energy per bond is 112.25 kJ/mol, which is comparable to the $C_{60}H_{10}-C_5H_{11}$ binding energy. This suggests that, depending on the radical sites on the polymer chains, many covalent bonds may form with the nanotube at multiple sites. However, the steric hindrance between the polymer chains that attach to the nanotube will limit the process.

The reaction of the biradical (Model IV) with either a $CH_3$ radical or an $H^\bullet$ is energetically favorable. The optimized geometry of the $C_{60}H_{10}-C_7H_{14}-CH_3$ radical showing three covalent bonds with the nanotube is given in Figure 6. The calculated binding energy of the $CH_3$ radical to the biradical is 232.7 kJ/mol, which is much higher than the binding energy of the $C_5H_{11}$ radical to the nanotube segment $C_{60}H_{10}$. This is because, in the latter, one of the $\pi$ bonds of the nanotube segment has to open up and a trigonal carbon should change into a tetrahedral carbon in order to form the new C−C bond, whereas the reaction of biradical with either a $CH_3$ radical or an $H^\bullet$ only requires the deformation of a sp$^2$ carbon into a sp$^3$ carbon as it is a combination reaction.

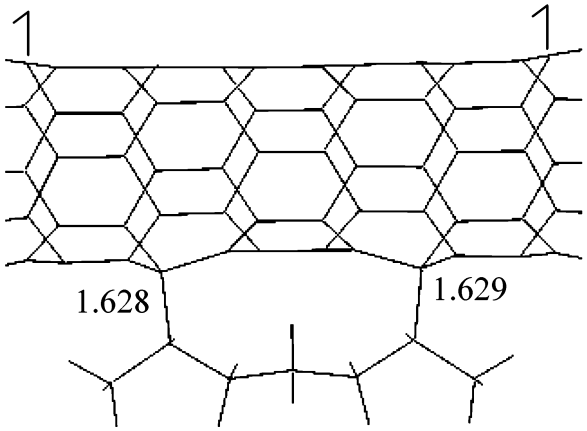

**Figure 5.** DFT(B3LYP)/3-21G-optimized geometry of the $C_{60}H_{10}-C_7H_{14}$ biradical.

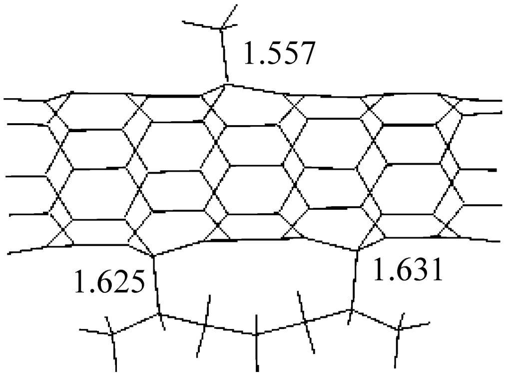

**Figure 6.** DFT(B3LYP)/3-21G-optimized geometry of the $C_{60}H_{10}-C_7H_{14}-CH_3$ radical.

Upon examination of the reactions of the $C_{60}H_{10}-C_7H_{14}$ biradical with a saturated polymer chain $C_5H_{12}$, we find that the abstraction of either a hydrogen atom from $C_5H_{12}$, leaving a $C_5H_{11}$ radical in the reaction mixture, or a $CH_3$ radical that leads to the formation of $C_{60}H_{10}-C_7H_{14}-CH_3$ radical, leaving $C_4H_9$ radical in the mixture, are not energetically favorable, as the products have high energy ($>$150 kJ/mol) compared to the reactants.

The above calculations on model systems shows that a polyethylene chain having radicals may form stronger covalent bonds with smaller diameter nanotubes. Hence, as stated in section 1, polyethylene may be reinforced by nanotubes using free-radical generators such as peroxide.

The commonly used experimental methods[4,30] to incorporate carbon nanotubes into a polymer matrix are direct mixing, in situ polymerization, solution mixing, and melt processing. Except the first one, the other three can be used for thermoplastic polymers. In Tang et al.'s work[4] on carbon nanotubes/HDPE, the melt-processing method was used. Polyethylene resins are generally produced by free-radical polymerization. Therefore, adding nanotubes in the in situ polymerization may also reinforce the polymer due to the possible formation of covalent bonds between the nanotubes and the growing polymer chains in the reaction mixture.

## 4. Conclusion

We have demonstrated that (i) covalent bond formation between alkyl radicals and carbon nanotubes is energetically favorable, (ii) the reaction may take place at multiple sites of nanotubes, and (iii) the reaction is more favorable with tubes of a small diameter. As alkyl radicals are good representatives of polyethylene chain radicals, it may be possible to form multiple covalent bonds between polyethylene chain radicals and nanotubes. Hence one way to improve the load transfer of carbon nanotube/HDPE composite via chemical bonds at the interface is to use free-radical generators such as peroxide or incorporate nanotubes in the in situ polymerization. The latter offers a direct guideline based on an established free-radical polymerization scheme for making composites with strong carbon nanotube−polyethylene interfaces and high-stress transfer ability.

**Acknowledgment.** The authors thank the Australian Research Council for the continuous financial support. This work was also supported by the Australian partnership for advanced computing. K.M. acknowledges the valuable discussion with Dr. G. Bacskay at the School of Chemistry.

## References and Notes

(1) Roelof, M.; Antonius, V. E. M. In *PCT Int. Appl.*, 2003.

(2) Marc, D.; Jacques, M. In *Eur. Pat. Appl.*, 2000.

(3) Ruan, S. L.; Gao, P.; Yang, X. G.; Yu, T. X. *Polymer* **2003**, *44*, 5643.

(4) Tang, W.; Santare, M. H.; Advani, S. G. *Carbon* **2003**, *41*, 2779.

(5) Ren, Y.; Li, F.; Cheng, H.-M.; Liao, K. *Carbon* **2003**, *41*, 2177.

(6) Bower, C.; Rosen, R.; Jin, L. *Appl. Phys. Lett.* **1999**, *74*, 3317.

(7) Schadler, L. S.; Giannaris, S. C.; Ajayan, P. M. *Appl. Phys. Lett.* **1998**, *73*, 3842.

(8) Xu, X.; Thwe, M. M. *Appl. Phys. Lett.* **2002**, *81*, 2833.

(9) Jia, Z.; Wang, Z.; Xu, C.; Liang, J.; Wei, B.; Wu, D.; Zhu, S. *Mater. Sci. Eng.* **1999**, *A271*, 395.

(10) Lau, K.-T.; Hui, D. *Carbon* **2002**, *40*, 1605.

(11) Lau, K.-T.; Shi, S.-Q. *Carbon* **2002**, *40*, 2961.

(12) Frankland, S. J. V.; Harik, V. M. *Surf. Sci. Lett.* **2003**, *525*, L103.

(13) Frankland, S. J. V.; Harik, V. M.; Odegard, G. M.; Brenner, D. W.; Gates, T. S. *Comput. Sci. Technol.* **2003**, *63*, 1655.

(14) Frankland, S. J. V.; Caglar, A.; Brenner, D. W.; Griebel, M. *J. Phys. Chem. B* **2002**, *106*, 3046.

(15) Wei, C.; Srivastava, D.; Cho, K. *Nano Lett.* **2002**, *2*, 647.

(16) Hamwi, A.; Alvergnat, H.; Bonnamy, S.; Beguin, F. *Carbon* **1997**, *35*, 723.

(17) Mickelson, E. T.; Chiang, I. W.; Zimmerman, J. L.; Boul, P. J.; Lozano, J.; Liu, J.; Smalley, R. E.; Hauge, R. H.; Margrave, J. L. *J. Phys. Chem. B* **1999**, *103*, 4318.

(18) Bauschlicher, C. R. *Chem. Phys. Lett.* **2000**, *322*, 237.

(19) Bauschlicher, C. W. *Nano Lett.* **2001**, *1*, 223.

(20) Jaffe, R. L. *J. Phys. Chem. B* **2003**, *107*, 10378.

(21) Patil, A. O.; Brois, S. J. *Polymer* **1997**, *38*, 3423.

(22) Becke, A. D. *Phys. Rev. A* **1988**, *38*, 3098.

(23) Lee, C.; Yang, W.; Parr, R. G. *Phys. Rev. B* **1988**, *37*, 785.

(24) Vosko, S. H.; Wilk, L.; Nusair, M. *Can. J. Phys.* **1980**, *58*, 1200.

(25) Becke, A. D. *J. Chem. Phys.* **1993**, *98*, 5648.

(26) Binkley, J. S.; Pople, J. A.; Hehre, W. J. *J. Am. Chem. Soc.* **1980**, *102*, 939.

(27) Mulliken, R. S. *J. Chem. Phys.* **1955**, *23*, 1833.

(28) D'Souza, F.; Zandler, M. E.; Smith, P. M.; Deviprasad, G. R.; Arkady, K.; Fujitsuka, M.; Ito, O. *J. Phys. Chem. A* **2002**, *106*, 649.

(29) Frisch, M. J.; Trucks, G. W.; Schlegel, H. B.; Scuseria, G. E.; Robb, M. A.; J. R. Cheeseman, J. A. M., Jr.; Vreven, T.; Kudin, K. N.; Burant, J. C.; Millam, J. M.; Iyengar, S. S.; Tomasi, J.; Barone, V.; Mennucci, B.; Cossi, M.; Scalmani, G.; Rega, N.; Petersson, G. A.; Nakatsuji, H.; Hada, M.; Ehara, M.; Toyota, K.; Fukuda, R.; Hasegawa, J.; Ishida, M.; Nakajima, T.; Honda, Y.; Kitao, O.; Nakai, H.; Klene, M.; Li, X.; Knox, J. E.; Hratchian, H. P.; Cross, J. B.; Adamo, C.; Jaramillo, J.; Gomperts, R.; Stratmann, R. E.; Yazyev, O.; Austin, A. J.; Cammi, R.; Pomelli, C.; Ochterski, J. W.; Ayala, P. Y.; Morokuma, K.; Voth, G. A.; Salvador, P.; Dannenberg, J. J.; Zakrzewski, V. G.; Dapprich, S.; Daniels, A. D.; Strain, M. C.; Farkas, O.; Malick, D. K.; Rabuck, A. D.; Raghavachari, K.; Foresman, J. B.; Ortiz, J. V.; Cui, Q.; Baboul, A. G.; Clifford, S.; Cioslowski, J.; Stefanov, B. B.; Liu, G.; Liashenko, A.; Piskorz, P.; Komaromi, I.; Martin, R. L.; Fox, D. J.; Keith, T.; Al-Laham, M. A.; Peng, C. Y.; Nanayakkara, A.; Challacombe, M.; Gill, P. M. W.; Johnson, B.; Chen, W.; Wong, M. W.; Gonzalez, C.; Pople, J. A.; *Gaussian 03*, Revision A.1; Gaussian, Inc.: Pittsburgh, PA, 2003.

(30) Jin, Z.; Pramoda, K. P.; Goh, S. H.; Xu, G. *Mater. Res. Bull.* **2002**, *37*, 271.